



HAL
open science

A new elastoviscoplastic model based on the Herschel-Bulkley viscoplasticity

Pierre Saramito

► **To cite this version:**

Pierre Saramito. A new elastoviscoplastic model based on the Herschel-Bulkley viscoplasticity. 2008.
hal-00316158v1

HAL Id: hal-00316158

<https://hal.science/hal-00316158v1>

Preprint submitted on 2 Sep 2008 (v1), last revised 2 Dec 2008 (v3)

HAL is a multi-disciplinary open access archive for the deposit and dissemination of scientific research documents, whether they are published or not. The documents may come from teaching and research institutions in France or abroad, or from public or private research centers.

L'archive ouverte pluridisciplinaire **HAL**, est destinée au dépôt et à la diffusion de documents scientifiques de niveau recherche, publiés ou non, émanant des établissements d'enseignement et de recherche français ou étrangers, des laboratoires publics ou privés.

A new elastoviscoplastic model based on the Herschel-Bulkley viscoplasticity

Pierre Saramito

September 2, 2008

Abstract – The aim of this paper is to introduce a new three-dimensional elastoviscoplastic model that combines both the Oldroyd viscoelastic model and the Heshell-Bulkley viscoplastic model with a power-law index $n > 0$. The present model is founded to satisfy the second law of thermodynamics. Various fluids of practical interest, such as liquid foams, droplet emulsions or blood, present such elastoviscoplastic behavior: at low stress, the material behaves as a viscoelastic solid, whereas at stresses above a yield stress, the material behaves as a fluid. When $n = 1$, a recently introduced elastoviscoplastic model proposed by the author is obtained. When $0 < n < 1$, then the plasticity criteria becomes smooth, the elongational viscosity is always well defined and the shear viscosity shows a shear thinning behavior : this is a major improvement to the previous elastoviscoplastic model. Finally, when $n > 1$, the material exhibits the less usual shear thickening behavior.

Keywords – non-Newtonian fluid; viscoelasticity; viscoplasticity; constitutive equation.

1 Introduction

In 1926, Hershel and Bulkley [6] proposed a power law variant of the original viscoplastic Bingham model [1] :

$$\begin{cases} |\tau| \leq \tau_0 & \text{when } \dot{\varepsilon} = 0 \\ \tau = k|\dot{\varepsilon}|^{n-1}\dot{\varepsilon} + \tau_0 \frac{\dot{\varepsilon}}{|\dot{\varepsilon}|} & \text{otherwise} \end{cases} \iff \max\left(0, \frac{|\tau| - \tau_0}{k|\tau|^n}\right)^{\frac{1}{n}} \tau = \dot{\varepsilon}$$

where τ is the stress, $\dot{\varepsilon}$ the rate of deformation, $k > 0$ the consistency parameter and $\tau_0 > 0$ the yield stress. Remark that $k|\dot{\varepsilon}|^{n-1}$ has the dimension of a viscosity. Here, $n > 0$ is the power index. When $n = 1$ the model reduced to the Bingham model. The shear thinning behavior is associated to $0 < n < 1$ and the less usual shear thickening behavior to $n > 1$. In 2007, by introducing viscoelasticity in a viscoplastic model, a three-dimensional combination of the viscoelastic Oldroyd and viscoplastic Bingham model has been introduced [17] and studied in the context of liquid foam [2]. The aim of this paper is to explore the elastoviscoplastic extension of the Hershel and Bulkley model, that writes in one-dimensional form:

$$\frac{1}{\mu}\dot{\tau} + \max\left(0, \frac{|\tau| - \tau_0}{k|\tau|^n}\right)^{\frac{1}{n}} \tau = \dot{\varepsilon} \quad (1)$$

where $\mu > 0$ is the elasticity parameter and $\sigma = \tau + \eta\dot{\varepsilon}$ is the total stress, where $\eta > 0$ is a viscosity, often called the solvent viscosity in the context of polymer melts. When $n = 1$ and $\tau_0 = 0$ we obtain a one-dimensional version of the Oldroyd viscoelastic model [14]. This model is motivated by the existence

of material that present elastic solid-like behavior at low stress and power-index shear thinning behavior fluid-like at high stress. In 1988, Ketz et al. [9] identified elasticity moduli and yield stress values for concentrated Carbopol micro-gel dispersions, and then, Piau [15] estimated the corresponding power law index $n = 0.37$. Based on experimental measurements, Katgert et al. [8] estimated recently the power index value of the Hershel-Bulkley model for liquid foams to $n = 0.36$, while Langlois et al. [10, 19], based on a direct numerical simulation of liquid foams, proposed $n = 0.54$. Biological flows containing cells [7] leads also to n varying from 0.5 to 1 depending on the cell concentration. Notice also that Laun (see [11, p. 265] and related references) points out the less usual shear thickening behavior ($n > 1$ case) for suspensions of solid particles.

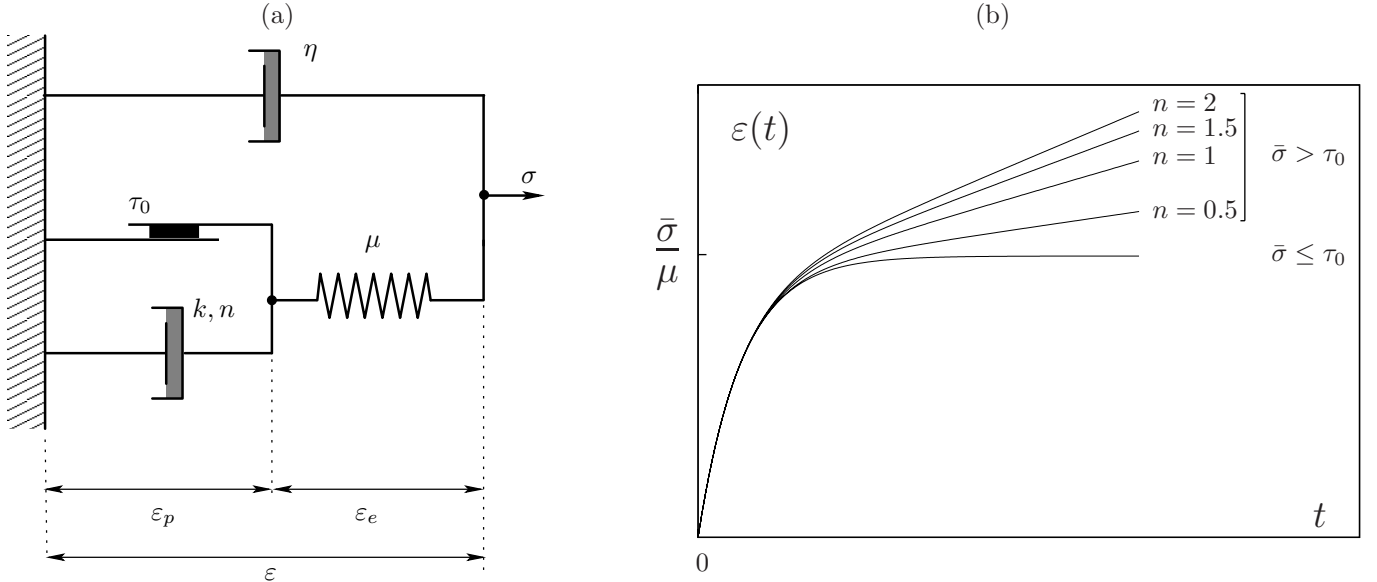


Figure 1: Creeping test for the present model.

The mechanical model is represented in Fig. 1.a. At stresses below the yield stress, the friction element remains rigid. The level of the elastic strain energy required to break the friction element is determined by the von Mises yielding criterion. Consequently, before yielding, the whole system predicts only recoverable Kelvin-Voigt viscoelastic deformation due to the spring μ and the viscous element η . The elastic behavior $\tau = \mu\varepsilon$ is expressed in (1) in differential form. Before yielding, the total stress is $\sigma = \mu\varepsilon + \eta\dot{\varepsilon}$. As soon as the strain energy exceeds the level required by the von Mises criterion, the stress in the friction element attains the yield value and the element breaks allowing deformation of all the other elements. After yielding, the deformation of these elements describes a non-linear viscoelastic behavior.

The evolution in time of elongation $\varepsilon(t)$ for a fixed imposed traction $\bar{\sigma}$ (creeping) is represented on Fig 1.b. When $\bar{\sigma} \leq \tau_0$, the elongation for a fixed imposed traction is bounded in time, which means that such material behaves as a solid. Otherwise, $\bar{\sigma} > \tau_0$, the elongation is unbounded in time, which means that the material behaves as a fluid.

The aim of the present article is to build the proposed model for the general three-dimensional case (section 2) and to study it on simple shear and extensional flows (section 3). The impatient reader – and the reader who is unfamiliar with the thermodynamic framework – could jump directly to the end of section 2 where the complete set of equations (7) governing such a flow is presented, before reading section 3 devoted to applications.

2 The proposed model

2.1 Thermodynamic framework

The state of the system is described by using two independent variables : the total deformation tensor ε and an internal variable, the elastic deformation tensor ε_e . We have $\varepsilon = \varepsilon_e + \varepsilon_p$ where ε_p represents the plastic deformation tensor. Following Halphen and Nguyen [5] (see e.g. [18] or [12, p. 97]) we say that a *generalized standard material* is characterized by the existence of a free energy function \mathcal{E} and a potential of dissipation \mathcal{D} , that are both convex functions of their arguments. The proposed model can be written as:

$$\begin{aligned}\mathcal{E}(\varepsilon, \varepsilon_e) &= \mu |\varepsilon_e|^2, \\ \mathcal{D}(\dot{\varepsilon}, \dot{\varepsilon}_e) &= \varphi(\dot{\varepsilon}) + \varphi_p(\dot{\varepsilon} - \dot{\varepsilon}_e),\end{aligned}\quad (2)$$

where $\mu > 0$ is the elasticity parameter and where $|\cdot|$ denotes the matrix norm, defined by a double contraction of indices : $|\varepsilon_e|^2 = \varepsilon_e : \varepsilon_e$. The functions φ and φ_p are expressed by :

$$\varphi(\dot{\varepsilon}) = \begin{cases} \eta |\dot{\varepsilon}|^2 & \text{when } \text{tr } \dot{\varepsilon} = 0, \\ +\infty & \text{otherwise,} \end{cases} \quad \text{and} \quad \varphi_p(\dot{\varepsilon}_p) = \begin{cases} \frac{2k}{n+1} |\dot{\varepsilon}_p|^{n+1} + \tau_0 |\dot{\varepsilon}_p| & \text{when } \text{tr } \dot{\varepsilon}_p = 0, \\ +\infty & \text{otherwise.} \end{cases} \quad (3)$$

When $n = 1$, the model coincides with the elastoviscoplastic model introduced in [17] that combines the Bingham and the Oldroyd models. The φ function expresses the incompressible viscous behavior and is associated to the viscosity $\eta \geq 0$ while the φ_p function expresses the viscoplastic behavior by using a power law index $n > 0$ and a consistency parameter $k > 0$, acting on continuous modification of the network links, and also a yield stress value $\tau_0 \geq 0$. When the stress becomes higher than this value, some topological modifications appear in the network of contacts. This model satisfies the second law of thermodynamics: in the framework of *generalized standard materials* [5, 18, 12] this property is a direct consequence of the convexity of both \mathcal{E} and \mathcal{D} .

2.2 The general constitutive law

Let Ω be a bounded domain of \mathbb{R}^N , where $N = 1, 2, 3$. Since both φ and φ_p are non-linear and non-differentiable, the following manipulations involve subdifferential calculus from convex analysis. The material constitutive laws can be written as:

$$\sigma \in \frac{\partial \mathcal{E}}{\partial \varepsilon} + \frac{\partial \mathcal{D}}{\partial \dot{\varepsilon}} \quad \text{and} \quad 0 \in \frac{\partial \mathcal{E}}{\partial \varepsilon_e} + \frac{\partial \mathcal{D}}{\partial \dot{\varepsilon}_e}, \quad (4)$$

where σ is the total Cauchy stress tensor. Using definition (2) of \mathcal{E} and \mathcal{D} , we get:

$$\sigma \in \partial \varphi(\dot{\varepsilon}) + \partial \varphi_p(\dot{\varepsilon} - \dot{\varepsilon}_e) \quad \text{and} \quad 0 \in 2\mu \varepsilon_e - \partial \varphi_p(\dot{\varepsilon} - \dot{\varepsilon}_e). \quad (5)$$

The combination of the two previous relations leads to $\sigma - 2\mu \varepsilon_e \in \partial \varphi(\dot{\varepsilon})$. Then, by using expression (11) of $\partial \varphi$ from the technical annex, and by introducing the pressure field p , we get the following expression of the total Cauchy stress tensor: $\sigma = -p.I + 2\eta \dot{\varepsilon} + 2\mu \varepsilon_e$ when $\text{tr}(\dot{\varepsilon}) = 0$. Then, the second relation in (5) is equivalent to $\dot{\varepsilon} - \dot{\varepsilon}_e \in \partial \varphi_p^*(2\mu \varepsilon_e)$ where φ_p^* is the dual of φ_p . Let us introduce the elastic stress tensor $\tau = 2\mu \varepsilon_e$. The expression (10) of $\partial \varphi_p^*$ in annex yields:

$$\frac{1}{2\mu} \dot{\tau} + \max \left(0, \frac{|\tau_d| - \tau_0}{2k |\tau_d|^{r-1}} \right)^{\frac{1}{n}} \tau = \dot{\varepsilon} \quad (6)$$

where $\tau_d = \tau - \frac{1}{N} \text{tr}(\tau) I$ denotes the deviatoric part of τ .

2.3 The system of equations

Since the material is considered in large deformations, we choose to use the Eulerian mathematical framework, more suitable for fluids flows computations. We assume that $\dot{\varepsilon} = D(\mathbf{v}) = (\nabla \mathbf{v} + \nabla \mathbf{v}^T)/2$ is the rate of deformation, while the material derivative $\dot{\tau}$ of tensor τ in the Eulerian framework is expressed by the Gordon-Schowalter derivative [4] : $\dot{\tau} = \frac{\square}{\partial t} \tau + \mathbf{v} \cdot \nabla \tau + \tau W(\mathbf{v}) - W(\mathbf{v})\tau - a(\tau D(\mathbf{v}) + D(\mathbf{v})\tau)$ where $W(\mathbf{v}) = (\nabla \mathbf{v} - \nabla \mathbf{v}^T)/2$ is the vorticity tensor. The material parameter $a \in [-1, 1]$ is associated to the Gordon-Schowalter's derivative. When $a = 0$ we obtain the Jaumann derivative of tensors, while $a = 1$ and $a = -1$ are associated to the upper and the lower convected derivatives, respectively.

The elastoviscoplastic fluid is then described by a set of three equations associated to three unknowns (τ, \mathbf{v}, p) : the differential equation (6) is completed with the conservation of momentum and mass:

$$\left\{ \begin{array}{l} \frac{1}{2\mu} \frac{\square}{\tau} + \max\left(0, \frac{|\tau_d| - \tau_0}{2k|\tau_d|^n}\right)^{\frac{1}{n}} \tau - D(\mathbf{v}) = 0, \\ \rho \left(\frac{\partial \mathbf{v}}{\partial t} + \mathbf{v} \cdot \nabla \mathbf{v} \right) - \mathbf{div} (-pI + 2\eta D(\mathbf{v}) + \tau) = \mathbf{f}, \\ \mathbf{div} \mathbf{v} = 0, \end{array} \right.$$

where ρ denotes the constant density and \mathbf{f} a known external force, such as the gravity. These equations are completed by some suitable initial and boundaries conditions in order to close the system. For instance the initial conditions $\tau(t=0) = \tau_0$ and $\mathbf{v}(t=0) = \mathbf{v}_0$ and the boundary condition $\mathbf{v} = 0$ on the boundary $\partial\Omega$ are convenient. The total Cauchy stress tensor can be written as:

$$\sigma = -pI + 2\eta D(\mathbf{v}) + \tau.$$

2.4 Dimensionless formulation

Let U, L be some characteristic velocity and length of the flow, respectively. Let us introduce $\eta_p = k(L/U)^{1-n}$, that has the dimension of a viscosity, and $\eta_0 = \eta + \eta_p$ that denotes the total viscosity. Let $\lambda = \eta_p/\mu$ that has the dimension of a time. Let $T = L/U$ and $\Sigma = (\eta + \eta_p)U/L$ be some characteristic time and stress, respectively. We introduce the following classical dimensionless numbers:

$$We = \frac{\lambda U}{L}, \quad Bi = \frac{\tau_0 L}{\eta_0 U} \quad \text{and} \quad Re = \frac{\rho U L}{\eta_0}$$

We use also the retardation parameter $\alpha = \eta_p/\eta_0 \in]0, 1]$. The problem reduces to that of finding dimensionless fields, also denoted by (τ, \mathbf{v}, p) such that:

$$\left\{ \begin{array}{l} We \frac{\square}{\tau} + \kappa_n(|\tau_d|) \tau - 2\alpha D(\mathbf{v}) = 0, \\ Re \left(\frac{\partial \mathbf{v}}{\partial t} + \mathbf{v} \cdot \nabla \mathbf{v} \right) - \mathbf{div} (-pI + 2(1 - \alpha)D(\mathbf{v}) + \tau) = \mathbf{f}, \\ \mathbf{div} \mathbf{v} = 0, \end{array} \right. \quad (7)$$

where κ_n denotes the plasticity criteria function :

$$\kappa_n(s) = \max\left(0, \frac{s - Bi}{(2\alpha)^{1-n} s^n}\right)^{\frac{1}{n}}, \quad \forall s \geq 0 \quad (8)$$

and \mathbf{f} denotes some known dimensionless vector field. These equations are completed by the initial and boundaries conditions. Notice that when $We = 0$ the model reduces to the viscoplastic Herschel-Bulkley

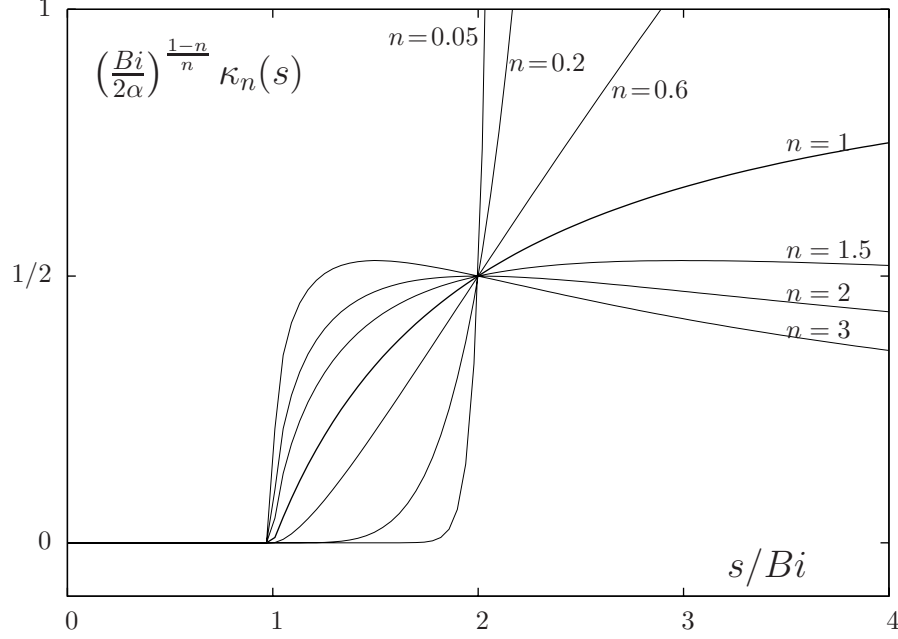


Figure 2: The Herschel-Bulkley plasticity criteria function κ_n for various n values.

model and when $Bi = 0$ and $n = 1$ it reduces to the usual viscoelastic Oldroyd model [13, 16]. When both $We = Bi = 0$ and $n = 1$ the fluid is Newtonian and the set of equations reduces to the classical Navier-Stokes equations. Conversely, when both $We \neq 0$ and $Bi \neq 0$ the fluid is elastoviscoplastic.

Fig. 2 plots the κ_n function for various values of n . Observe the $\kappa_n(s)$ behavior at $s = Bi$. The function is continuous and its left derivative is zero while its right derivative is also zero when $n < 1$, it is $1/Bi$ when $n = 1$ and $+\infty$ when $n > 1$. As a consequence, the function is smooth, i.e. its derivative is continuous, at $s = Bi$ if and only if $0 < n < 1$. Observe also that, when $0 < n < 1$, then κ_n is unbounded. Conversely, when $n \geq 1$, then κ_n is bounded in \mathbb{R}^+ by a value denoted by κ_n^* that depend upon n , Bi and α . More precisely, the derivative writes:

$$\kappa_n'(s) = \frac{(s - Bi)^{\frac{1-n}{n}}}{(2\alpha)^{\frac{1-n}{n}} s^2} \left(Bi + \left(\frac{1-n}{n} \right) s \right), \quad \forall s > Bi$$

and then, for $n \geq 1$, then κ_n reaches its maximum κ_n^* at $s^* = \left(\frac{n}{n-1} \right) Bi$ and

$$\kappa_n^* = \begin{cases} 1 & \text{when } n = 1 \\ \left(\frac{2\alpha}{Bi} \right)^{\frac{n-1}{n}} \frac{(n-1)^{\frac{n-1}{n}}}{n} & \text{when } n > 1 \end{cases}$$

These basic properties of κ_n are essential when studying the model on practical examples. This is the subject of the following paragraph.

3 Examples

3.1 Uniaxial elongation

The fluid is at the rest at $t = 0$ and a constant elongational rate $\dot{\epsilon}_0$ is applied: the Weissenberg number is $We = \lambda\dot{\epsilon}_0$ and the Bingham number $Bi = \tau_0/(\eta_0\dot{\epsilon}_0)$. All quantities presented in this paragraph are dimensionless.

The flow is three-dimensional and the dimensionless velocity gradient writes $\nabla\mathbf{v} = \text{diag}(1, -1/2, -1/2)$. The problem reduces to find τ_{11}, τ_{22} and τ_{33} such that

$$\begin{cases} We \frac{d\tau_{11}}{dt} + (\kappa_n(|\tau_d|) - 2aWe)\tau_{11} = 2\alpha, \\ We \frac{d\tau_{jj}}{dt} + (\kappa_n(|\tau_d|) + aWe)\tau_{jj} = -\alpha, \quad j = 2, 3 \end{cases}$$

with the initial condition $\tau(t=0) = 0$. Since $\tau_{33} = \tau_{22}$ we have: $|\tau_d| = (2/3)^{1/2} |\tau_{11} - \tau_{22}|$. Since $\tau(0) = 0$ and $\tau(t)$ is continuous, there exists $t_0 > 0$ such that when $t \in [0, t_0]$ we have $|\tau_d| \leq Bi$ and thus $\kappa = 0$: this is the linear flow regime. The eigenvalues of the system are $-2aWe$ and aWe . For $t > t_0$, the case $\kappa_n(|\tau_d|) > 0$ occurs. When $n \geq 1$, since κ_n is bounded by κ_n^* , when $aWe > \kappa_n^*/2$ the stress becomes unbounded in finite time, as shown on Fig. 3.a that plots the dimensionless first normal stress difference $\tau_{11} - \tau_{22}$. Conversely,

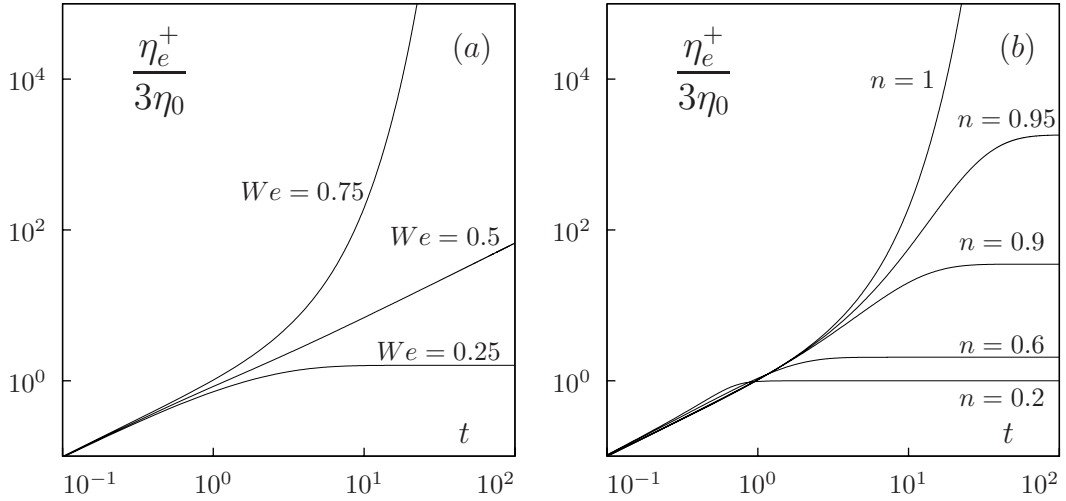


Figure 3: Dimensionless first normal stress difference $\tau_{11} - \tau_{22}$ for uniaxial elongation when $Bi = 1$, $a = 1$ and $\alpha = 1$: (a) influence of We for $r = 2$; (b) influence of n for $We = 0.75$.

when $0 < n < 1$, since κ_n is strictly increasing and unbounded in \mathbb{R}^+ , the factor $\kappa_n(|\tau_d|) - 2aWe$ remains positive for large $|\tau_d|$. Then the system is amortized and the solution remains always bounded. This feature when $0 < n < 1$ is an important improvement to the case $n = 1$ that was previously considered in [17].

The stationary problem reduces to find τ_{11} and τ_{22} such that

$$\begin{cases} (\kappa_n(|\tau_d|) - 2aWe)\tau_{11} = 2\alpha \\ (\kappa_n(|\tau_d|) + aWe)\tau_{22} = -\alpha \end{cases}$$

When $a = 0$ the stationary solution is independent of We and $\psi = (\tau_{11} - \tau_{22})/2$ satisfies: $\kappa_n(|\tau_d|)\psi = 3\alpha/2$. Then $\psi \geq 0$ and $|\tau_d| = \sqrt{8/3} \psi$. The previous equation leads to the following explicit expression of the elongational viscosity:

$$\frac{\eta_e}{3\eta_0} = 1 - \alpha + (2/3)\psi = 1 - \alpha + (2/3)^{\frac{1-n}{2}}\alpha + (2/3)^{\frac{1}{2}}Bi$$

Remark that when $a = 0$, $n = 1$ and $Bi = 0$, we obtain the classical result $\eta_e = 3\eta_0$ i.e. the elongational viscosity in the Newtonian case is three times the total viscosity.

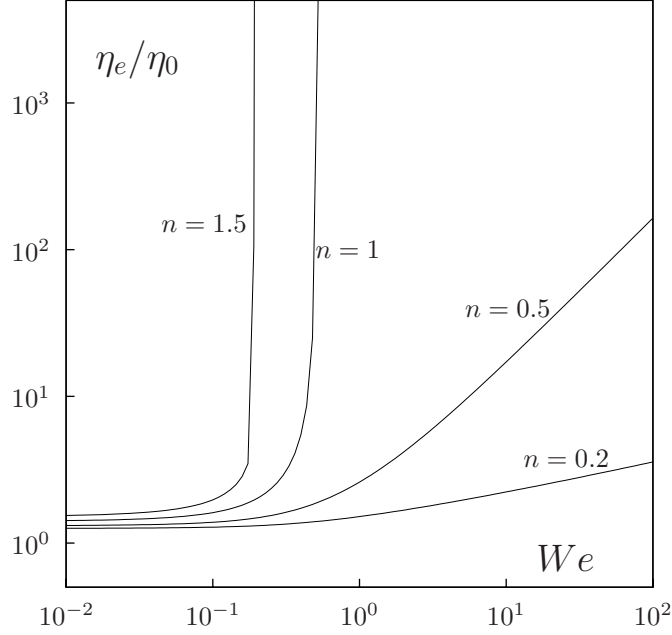


Figure 4: Elongational viscosity for $a = 1$, $Bi = 1$, $\alpha = 1$.

Fig. 4 plots the elongational viscosity when $a = 1$. The computation is no more explicit for a general $a \neq 0$ and requires a numerical resolution. We observe that its depend upon We , while it was independent of We when $a = 0$. Moreover, when $n \geq 1$, there exists a critical value of We upon which the elongational viscosity is no more defined. Conversely, when $0 < n < 1$, the elongational viscosity is defined for any We and is an increasing function of We .

3.2 Simple shear flow

The fluid is at the rest at $t = 0$ and a constant shear rate $\dot{\gamma}_0$ is applied: the Weissenberg number is $We = \lambda\dot{\gamma}_0$ and the Bingham number $Bi = \tau_0/(\eta_0\dot{\gamma}_0)$.

The flow is two-dimensional and the dimensionless velocity gradient is constant: $\nabla\mathbf{v} = ([0, 1]; [0, 0])$. The problem reduces to finding τ_{11}, τ_{22} and τ_{12} , such that, for all $t > 0$:

$$We \frac{d}{dt} \begin{pmatrix} \tau_{11} \\ \tau_{22} \\ \tau_{12} \end{pmatrix} + (We\mathcal{A}_a + \kappa_n(|\tau_d|).I) \begin{pmatrix} \tau_{11} \\ \tau_{22} \\ \tau_{12} \end{pmatrix} = \begin{pmatrix} 0 \\ 0 \\ \alpha \end{pmatrix},$$

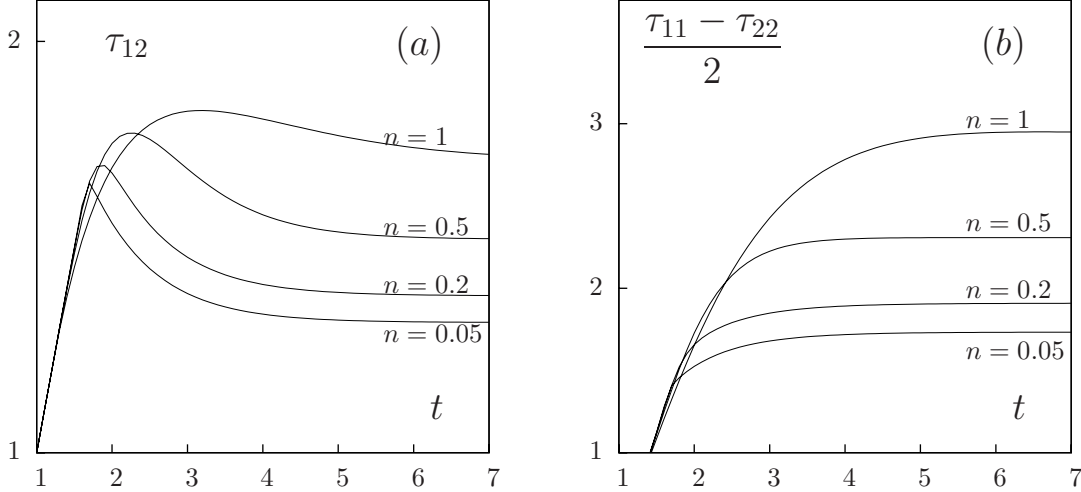


Figure 5: Simple shear flow for $a = 1$, $We = 1$, $Bi = 1$ and $\alpha = 1$: (a) τ_{12} ; (b) $(\tau_{11} - \tau_{22})/2$.

with the initial condition $\tau(0) = 0$, where

$$\mathcal{A}_a = \begin{pmatrix} 0 & 0 & -(1+a) \\ 0 & 0 & 1-a \\ \frac{1-a}{2} & -\frac{1+a}{2} & 0 \end{pmatrix}$$

with the initial condition $\tau(0) = 0$ and where $|\tau_d|^2 = (1/2)(\tau_{11} - \tau_{22})^2 + 2\tau_{12}^2$. Let $\psi = (\tau_{11} - \tau_{22})/2$ be the dimensionless normal stress difference. Then $\tau_{11} = \frac{1+a}{2}\psi$ and $\tau_{22} = -\frac{1-a}{2}\psi$. The solution (τ_{12}, ψ) is represented on Fig. 5. Since $\tau(0) = 0$ and $\tau(t)$ is continuous, there exists $t_0 > 0$ such that when $t \in [0, t_0]$ we have $|\tau_d| \leq Bi$ and thus $\kappa_n(|\tau_d|) = 0$: this is the linear flow regime. The eigenvalues of the system are 0 and $\pm i\sqrt{1-a^2}$. At $t = t_0$, $|\tau_d|$ reaches Bi . Then, for $t > t_0$, the non-linear factor $\kappa_n(|\tau_d|) > 0$ occurs: the corresponding term reduces the growth of the solution, which now remains bounded for any $n > 0$.

When $a = 1$ (see Fig. 5, where $\tau_{22} = 0$) the solution tends to a constant for any $Bi \geq 0$. Observe on Fig. 5.a that τ_{12} presents an overshoot that is more pronounced for small values of n . Conversely, $\tau_{11} - \tau_{22}$ is monotonically increasing for any values of n (Fig. 5.b). Let us observe on Fig. 6 the steady shear viscosity η_s/η_0 as a function of We . Notice that the dimensionless steady shear viscosity η_s/η_0 coincides with the dimensionless steady shear stress $\sigma_{12} = 1 - \alpha + \tau_{12}$. The material presents a shear thinning character when $0 < n < 1$ and a shear thickening character when $n > 1$. This feature is a second major improvement to the case $n = 1$ that was previously considered in [17]. For large We , the shear viscosity decreases monotonically when $0 < n < 1$ (Fig. 6.a), tends to a plateau when $n = 1$ (Fig. 6.b) and increases monotonically when $n > 1$ (Fig. 6.c). The value of Bi controls the viscosity plateau at small values of We while it has less influence on the viscosity for large values of We .

When $a = 0$ and Bi is small enough (see Fig. 7.a, where $\tau_{22} = -\tau_{11}$), the solution tends also to a constant with amortized oscillations. These oscillations are due to presence of complex eigenvalues in the system. When $a = 0$ and Bi becomes large, oscillations are no more amortized and instabilities appear, while the solution remains bounded (Fig. 7.b). The Lissajou plot on Fig. 8 shows the asymptotical orbit of the solution for various values of n . The orbit tangents the von Mises circle associated to $|\tau_d| = Bi$ (dotted lines). When the trajectory enters in the von Mises circle, the trajectory is exactly a circle, since the equations are linear

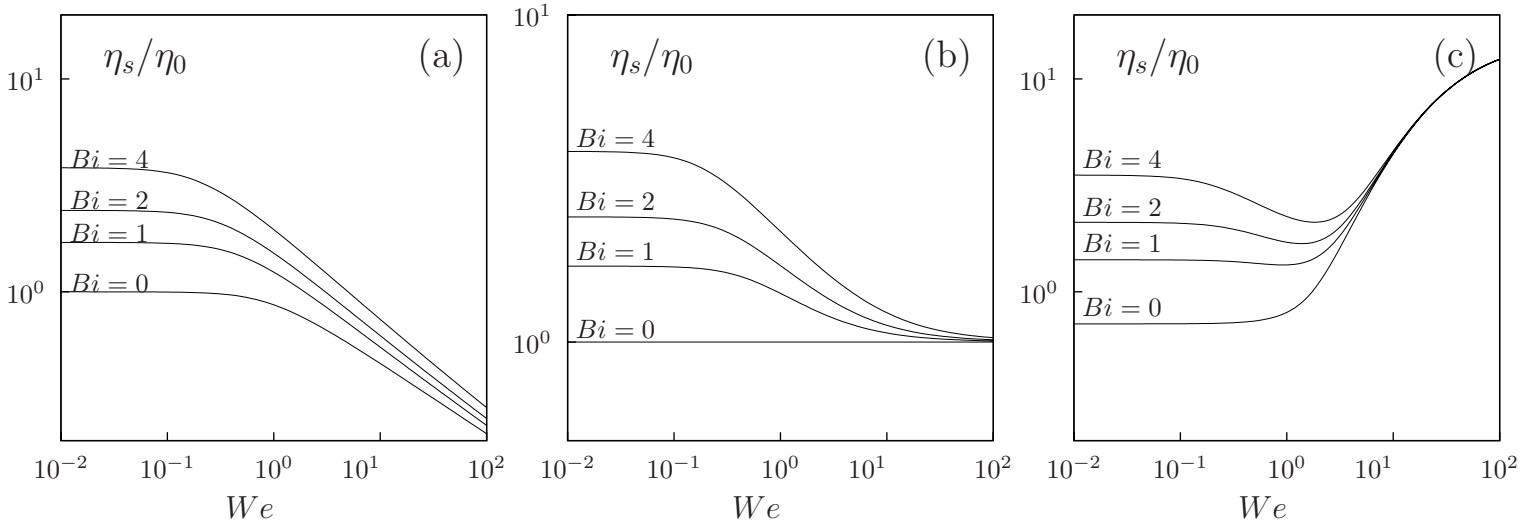


Figure 6: Shear viscosity for $a = 1$, $\alpha = 1$ and (a) $n = 0.5$; (b) $n = 1$; (c) $n = 1.5$.

when $\kappa_n(|\tau_d|) = 0$, while when it goes outside the circle, it is amortized, since the equations are non-linear. and $\kappa_n(|\tau_d|) > 0$. The asymptotical orbit is then completely included in the von Mises circle. We observe that the orbit in the Lissajou plot satisfies :

$$\tau_{12} = R_0 \sin(\omega t + \varphi) \quad \text{and} \quad \psi = \frac{\tau_{11} - \tau_{22}}{2} = 1 + R_0 \cos(\omega t + \varphi)$$

where R_0 is the radius of the orbit and φ is the phase shift that depends upon the initial value. The von Mises criteria for the asymptotical orbit writes $\max_t |\tau_d(t)| = Bi$ i.e.:

$$\max_t (1 + R_0 \cos(\omega t))^2 + (R_0 \sin(\omega t))^2 = Bi^2/2$$

and thus $R_0 = Bi/\sqrt{2} - 1$. Finally, the asymptotical orbit is a circle of radius R_0 and center $(\tau_{12}, \psi) = (0, 1)$ on the Lissajou plane. The power-law parameter n does no change the orbit: it changes the velocity of depreciation, as shown on 8. Finally, the critical Bingham number upon which instabilities are no more amortized is $Bi_c = \sqrt{2}$. The shear viscosity η_s is no more defined when $a = 0$ and We becomes large, since the solution for simple shear flow is no more stationary.

4 Conclusion

A new model for elastoviscoplastic fluid flows that is objective and satisfies the second law of thermodynamics is proposed in (7). It extends the previous elastoviscoplastic model introduced in [17] by introducing a power law index $n > 0$. As a major improvement, when $0 < n < 1$ this model presents finite extensional properties and a shear thinning behavior. As many elastoviscoplastic material has been founded to present a shear thinning behavior, this model is a good candidate for numerical simulation of such materials in complex multi-dimensional geometries (see e.g. [3]) and future work will focus on quantitative comparisons between experimental measurements and numerical predictions, as it was initiated in [2].

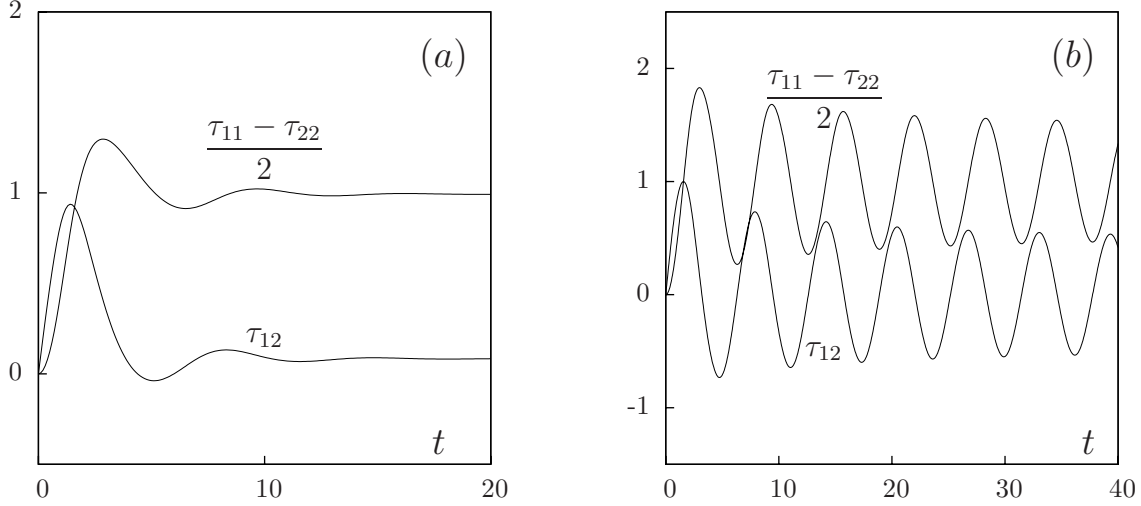


Figure 7: Simple shear flow for $a = 0$, $n = 0.5$, $We = 1$ and $\alpha = 1$: (a) $Bi = 1$; (b) $Bi = 2$.

A Technical annex

A.1. *The φ_p function* – The subgradient $\partial\varphi_p$, as introduced in (3), is defined for any tensor D by:

$$\begin{aligned}\partial\varphi_p(D) &= \{\tau, \tau : (H - D) \leq \varphi_p(H) - \varphi_p(D), \forall H\} \\ &= \{\tau, j_p(D) \leq j_p(H), \forall H \text{ with } \text{tr}(H) = 0 \text{ and } \text{tr}(D) = 0\},\end{aligned}$$

with the notation $j_p(H) = \frac{2k}{n+1}|H|^{n+1} + \tau_0|H| - \tau : H$. When the minimizer D of j_p over the set $\{D, \text{tr} D = 0\}$ is non vanishing, it satisfies, from the theory of Lagrange multipliers:

$$\nabla j_p(D) - p.I = 0 \text{ and } \text{tr}(D) = 0,$$

where p is the Lagrange multiplier. Then $2k|D|^{n-1}D + \tau_0 \frac{D}{|D|} - \tau - p.I = 0$ and $\text{tr}(D) = 0$. Thus the subgradient finally writes:

$$\partial\varphi_p(D) = \begin{cases} \{\tau, |\tau_d| \leq \tau_0\} & \text{when } D = 0, \\ \left\{ \tau, \tau = -p.I + 2k|D|^{n-1}D + \tau_0 \frac{D}{|D|} \right\} & \text{when } D \neq 0 \text{ and } \text{tr}(D) = 0, \\ \emptyset & \text{otherwise,} \end{cases} \quad (9)$$

where τ_d denotes the deviatoric part of τ . The dual φ_p^* of φ_p is then characterized by the Fenchel identity, that is, for any $\tau \in \partial\varphi_p(D)$, by $\varphi_p^*(\tau) = \tau : D - \varphi_p(D)$. Moreover, $\tau \in \partial\varphi_p(D)$ is equivalent to $D \in \partial\varphi_p^*(\tau)$. From $\tau + p.I = (2k|D|^{n-1} + \tau_0/|D|)D$ we get $|\tau_d| = 2k|D|^n + \tau_0$ and thus $|D| = ((|\tau_d| - \tau_0)/(2k))^{1/n}$. Finally:

$$\partial\varphi_p^*(\tau) = \left\{ D, D = \max \left(0, \frac{|\tau_d| - \tau_0}{2k|\tau_d|^n} \right)^{1/n} \tau_d \right\}, \quad (10)$$

where τ_d denotes the deviatoric part of τ .

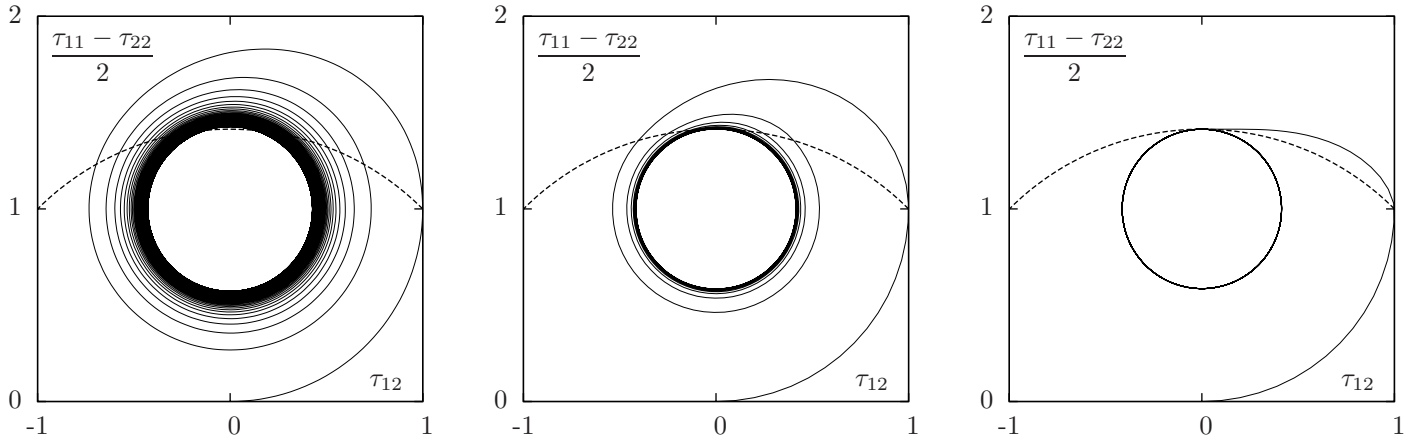


Figure 8: Simple shear flow when $a = 0$: flow instabilities and asymptotical orbit when (a) $n = 0.5$; (b) $n = 1$; (c) $n = 2$. The dotted line indicates the von Mises circle.

A.2. *The φ function* – The function φ , as introduced in (3), is a particular case of φ_p with $\tau_0 = 0$, $n = 1$ and $k = \eta$. From (9), the subgradient writes:

$$\partial\varphi(D) = \begin{cases} \{\tau, \tau = -p.I + 2\eta D\} & \text{when } \text{tr}(D) = 0, \\ \emptyset & \text{otherwise.} \end{cases} \quad (11)$$

References

- [1] E. C. Bingham. *Fluidity and plasticity*. Mc Graw-Hill, 1922.
- [2] I. Cheddadi, P. Saramito, C. Raufaste, P. Marmottant, and F. Graner. Numerical modelling of foam couette flows. *European Physical Journal - E. Soft matter*, **to appear**, 2008. <http://hal.archives-ouvertes.fr/hal-00240536>.
- [3] B. Dollet, M. Durth, and F. Graner. Flow of a foam past an elliptical obstacle. *Phys. Rev. E*, **73**, 2006.
- [4] R. J. Gordon and W. R. Schowalter. Anisotropic fluid theory: a different approach to the dumbbell theory of dilute polymer solutions. *Trans. Soc. Rheol.*, **16**:79–97, 1972.
- [5] B. Halphen and Q. S. NGuyen. Sur les matériaux standard généralisés. *J. Méca.*, **14**:39–63, 1975.
- [6] W. H. Herschel and T. Bulkley. Measurement of consistency as applied to rubber-benzene solutions. *Am. Soc. Test Proc.*, **26**(2):621–633, 1926.
- [7] A. Iordan, A. Duperray, and C. Verdier. Fractal approach to the rheology of concentrated cell suspensions. *Phys. Rev. E*, **77**:011911, 2008.
- [8] G. Katgert, M. E. Möbius, and M. van Hecke. Rate dependence and role of disorder in linearly sheared two-dimensional foams. submitted to *Phys. Rev. Letter*, 2008. <http://arxiv.org/pdf/0711.4024>.
- [9] R.J. Ketz, R.K. Prud’homme, and W.W. Graessly. Rheology of concentrated micro-gel solutions. *Rheol. Acta*, **27**:531–539, 1988.
- [10] V. J. Langlois, S. Hutzler, and D. Weaire. Rheological properties of the soft disk model of 2D foams. submitted, 2008.

- [11] R. G. Larson. *The structure and rheology of complex fluids*. Oxford University Press, 1999.
- [12] G. Maugin. *The thermomechanics of plasticity and fracture*. Cambridge University Press, 1992.
- [13] J. G. Oldroyd. On the formulation of rheological equations of states. *Proc. Roy. Soc. London, A* 200:523–541, 1950.
- [14] J.G. Oldroyd. A rational formulation of the equations of plastic flow for a Bingham solid. *Proc. Camb. Philos. Soc.*, 43:100–105, 1947.
- [15] J. M. Piau. Carbopol gels: elastoviscoplastic and slippery glasses made of individual swollen sponges. meso- and macroscopic properties, constitutive equations and scaling laws. *J. Non-Newtonian Fluid Mech.*, 144:1–29, 2007.
- [16] P. Saramito. Operator splitting for viscoelastic fluid with a differential constitutive law. *C. R. Acad. Sci. Paris, Série II*, t. 319, No. 3:267–270, 1994.
- [17] P. Saramito. A new constitutive equation for elastoviscoplastic fluid flows. *J. Non Newtonian Fluid Mech.*, 145(1):1–14, 2007.
- [18] P. Le Tallec. *Numerical analysis of viscoelastic problems*. Masson, France, 1990.
- [19] D. Weaire, S. Hutzler, V. J. Langlois, and R. J. Clancy. Velocity dependence of shear localisation in a 2D foam. submitted to *Phil. Mag. Lett.*, 2008.